

# RADIAL FORCE OF BEARINGLESS WOUND-ROTOR INDUCTION MOTOR

**Jumei Cai**

Department of Electrical Machines (IEM), Aachen Institute of Technology (RWTH Aachen)  
Aachen, NRW, 52056, Germany  
[caijumei@iem.rwth-aachen.de](mailto:caijumei@iem.rwth-aachen.de), [henneberger@rwth-aachen.de](mailto:henneberger@rwth-aachen.de)

**Gerhard Henneberger**

Department of Electrical Machines (IEM), Aachen Institute of Technology (RWTH Aachen)  
Aachen, NRW, 52056, Germany  
[caijumei@iem.rwth-aachen.de](mailto:caijumei@iem.rwth-aachen.de), [henneberger@rwth-aachen.de](mailto:henneberger@rwth-aachen.de)

## ABSTRACT

In this paper the radial force of a bearingless wound-rotor induction motor was first theoretically analyzed. Because of the asymmetrical flux distribution and rotating fields in the bearingless wound-rotor induction motor transient finite element method was used to compute the radial force. The influences of the bearing current and the eccentricity of the rotor on the radial force were studied.

## INTRODUCTION

The principle of bearingless machines bases on the superposition of two fields with different numbers of pole pairs, which results in a radial force. With different rotor structures the bearingless conception can be implemented with reluctance machines [1], induction machines [2], permanent magnet machines [3], etc. Because of the different rotor structure the form of the rotor field and its influences on the radial force in each type of bearingless machine are also different. In this paper the specialties of the fields in bearingless induction motors will be discussed.

A bearingless induction motor with squirrel cage rotor was developed [4]. The test results indicate that there is a closely coupling between the driving part and the levitation part. The reason is that the rotor field of a squirrel cage motor consists of two components, one is induced from the driving field and the other is induced from the bearing field. The second component can act with the bearing field together to generate an additional torque which influences the driving performance. This argumentation was confirmed by the computation results with transient finite element method (FEM) in [5]. The driving control and the levitation control for

such a bearingless induction motor are therefore coupled with each other, which results in complicate control system.

To solve this problem a bearingless wound-rotor induction motor was developed, whose rotor winding is wound with the same number of pole pairs as that of the driving winding. With this rotor structure the bearing current has no influence on the driving performance and the driving control can be decoupled from the levitation control [6].

In order to build the levitation control system for the bearingless wound-rotor induction motor, it is important to study the radial force, how the radial force is generated in the motor and which variables influence the value and the direction of the radial force. In this paper the radial force of the bearingless wound-rotor induction motor will be first theoretically analyzed and then computed with transient finite element method. The influences of the bearing current and the eccentricity of the rotor on the radial force will be discussed.

## THEORETICAL ANALYSIS

One of the specialties of bearingless induction motors is that the rotor field is induced from the air gap field. In order to avoid the induced rotor field having the component which has the same number of pole pairs as that of the bearing field, a bearingless wound-rotor induction motor was developed.

### **Bearingless Wound-rotor Induction Motor**

In the stator of the bearingless wound-rotor induction motor there are two windings, one is the 4-pole driving winding, the other is the 2-pole bearing winding. The

difference between this motor and the squirrel cage motor is that in this motor the rotor winding is wound in the rotor slots with the same number of pole pairs as that of the driving winding. So the induced rotor field is forced to have only one component which has the same number of pole pairs as that of the driving field. The rotor field can not act with the bearing field to generate an additional component of torque, because the two fields have different numbers of pole pairs. Therefore, the bearing field does not influence the driving performance.

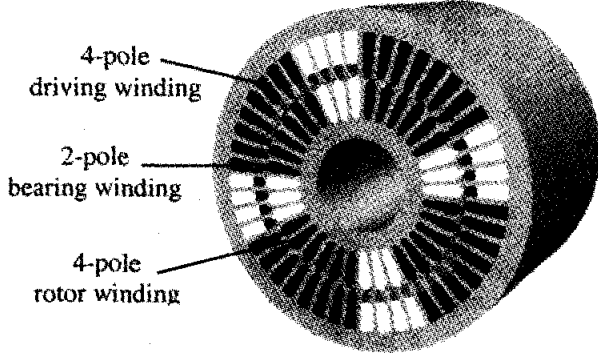


FIGURE 1: Bearingless wound-rotor induction motor

The form of the wound-rotor winding seems like the winding in a slip ring motor, but the rotor has no slip ring and this winding is short circuited and has no connection to the outside. The rotor structure is simple, robust and has no mechanical contact. Fig. 1 shows the structure of the bearingless wound-rotor induction motor.

### Radial Force

The generation of the radial force in bearingless machines is based on the superposition of fields with different numbers of pole pairs, which results in an asymmetrical flux distribution in the air gap. Another specialty of the bearingless induction motor is that all fields in the machine are rotating fields which are generated from the 3-phase currents in the driving winding, in the rotor winding and in the bearing winding. The 3-phase driving current, rotor current and bearing current can be described as following:

$$\begin{bmatrix} i_{1u} \\ i_{1v} \\ i_{1w} \end{bmatrix} = \begin{bmatrix} I_1 \cos \alpha t \\ I_1 \cos(\alpha t - \frac{2\pi}{3}) \\ I_1 \cos(\alpha t - \frac{4\pi}{3}) \end{bmatrix} \quad (1)$$

$$\begin{bmatrix} i_{2u} \\ i_{2v} \\ i_{2w} \end{bmatrix} = \begin{bmatrix} I_2 \cos(\alpha t - \varphi) \\ I_2 \cos(\alpha t - \varphi - \frac{2\pi}{3}) \\ I_2 \cos(\alpha t - \varphi - \frac{4\pi}{3}) \end{bmatrix} \quad (2)$$

$$\begin{bmatrix} i_{bu} \\ i_{bv} \\ i_{bw} \end{bmatrix} = \begin{bmatrix} I_b \cos(\alpha t + \beta) \\ I_b \cos(\alpha t + \beta - \frac{2\pi}{3}) \\ I_b \cos(\alpha t + \beta - \frac{4\pi}{3}) \end{bmatrix} \quad (3)$$

These currents generate three rotating fields, whose flux densities can be described as:

$$\begin{bmatrix} B_1(\alpha, t) \\ B_2(\alpha, t) \\ B_b(\alpha, t) \end{bmatrix} = \begin{bmatrix} \frac{3\mu_0 w_1}{2\pi\delta(\alpha)} I_1 \sin(2\alpha - \alpha t) \\ \frac{3\mu_0 w_2}{2\pi\delta(\alpha)} I_2 \sin(2\alpha - \alpha t + \varphi) \\ \frac{3\mu_0 w_b}{\pi\delta(\alpha)} I_b \sin(\alpha - \alpha t - \beta) \end{bmatrix} \quad (4)$$

Because both the driving winding and the rotor winding have 4 poles, the generated driving field and rotor field are both 4-pole rotating fields. The superposition of these two 4-pole fields is still a 4-pole rotating field. The bearing winding has 2 poles and the generated bearing field is a 2-pole rotating field. So in the motor it can be assumed that there exist a 4-pole field and a 2-pole field.

The air gap flux is the superposition of all these three rotating fields:

$$B_s(\alpha, t) = B_1(\alpha, t) + B_2(\alpha, t) + B_b(\alpha, t) \quad (5)$$

and the magnetic energy in the air gap:

$$W_m = \int \frac{B_s^2(\alpha, t)}{2\mu_0} I_{Fe} r \delta(\alpha) d\alpha \quad (6)$$

$$\delta(\alpha) = \delta_0 - dx \cos \alpha - dy \sin \alpha \quad (7)$$

If we use the approximation:

$$1/(1-x) \approx 1+x \quad (8)$$

for  $1/\delta(\alpha)$ , then we can get the radial force as following,

$$\begin{bmatrix} F_x \\ F_y \end{bmatrix} = \begin{bmatrix} \frac{\partial W_m}{\partial x} \\ \frac{\partial W_m}{\partial y} \end{bmatrix} = k_1 I_b \begin{bmatrix} I_1 \cos \beta + I_2 \cos(\varphi + \beta) \\ I_1 \sin \beta - I_2 \sin(\varphi + \beta) \end{bmatrix} \quad (9)$$

$$k_1 = \frac{9\mu_0^2 I_{Fe} r w_1 w_b}{4\pi\delta_0^2} \quad (10)$$

$$F = \sqrt{F_x^2 + F_y^2} = k_1 I_b \sqrt{I_1^2 + I_2^2 - 2I_1 I_2 \cos \varphi} \quad (11)$$

From the equivalent circuit diagram of the induction machine [7], it is known that

$$\bar{I}_1 = \bar{I}_2 + \bar{I}_0 \quad (12)$$

then equation (11) can be rewritten as:

$$F = \sqrt{F_x^2 + F_y^2} = k_1 I_b I_0 \quad (13)$$

$I_0$  is the magnetizing current as in the normal induction motor, here in the bearingless wound-rotor induction motor it is proportional to the total 4-pole flux.

From equation (13) it is known that the value of the radial force is dependent on the value of the bearing current and the total 4-pole flux. With the field oriented control for the driving part of the motor the 4-pole flux and the torque will be controlled independently to each other. The 4-pole field is constant in the fundamental speed range even though the load is changed. Hence, the value of the radial force is only proportional to the bearing current.

With the two-axis theory the bearing current can be described in rotating two-axis system as:

$$\begin{bmatrix} i_x \\ i_y \end{bmatrix} = \frac{\sqrt{6}}{2} I_b \begin{bmatrix} \cos \beta \\ \sin \beta \end{bmatrix} \quad (14)$$

In the field oriented control  $I_0$  can also be described in rotating two-axis system as  $I_\mu$ . Then from equations (9) and (13) the radial force can be rewritten as:

$$\begin{bmatrix} F_x \\ F_y \end{bmatrix} = F \begin{bmatrix} \cos \gamma \\ \sin \gamma \end{bmatrix} = k_1 I_0 I_b \begin{bmatrix} \cos \gamma \\ \sin \gamma \end{bmatrix}$$

$$\xrightarrow{\gamma = \beta!} = k_1 I_0 I_b \begin{bmatrix} \cos \beta \\ \sin \beta \end{bmatrix} = k_1' I_\mu \begin{bmatrix} i_x \\ i_y \end{bmatrix} \quad (15)$$

$$k_1' = k_1 \frac{2}{\sqrt{6}} \quad (16)$$

The equation (15) indicates that the direction of the radial force  $\gamma$  can be controlled by the phase angle between the bearing current and the driving current  $\beta$ , if the 4-pole field current keeps constant. Therefore, the radial force in x and y direction, namely  $F_x$  and  $F_y$  can be controlled by  $i_x$  and  $i_y$  respectively.

If we use the more approximate equation to calculate the radial force from the magnetic energy:

$$1/(1-x) = 1+x+x^2 \quad (17)$$

then we get another description of the radial force:

$$\begin{bmatrix} F_x \\ F_y \end{bmatrix} = \begin{bmatrix} \frac{\partial W_m}{\partial x} \\ \frac{\partial W_m}{\partial y} \end{bmatrix} = k_1 I_b \begin{bmatrix} I_1 \cos \beta + I_2 \cos(\varphi + \beta) \\ I_1 \sin \beta - I_2 \sin(\varphi + \beta) \end{bmatrix}$$

$$+ [k_2 (I_1^2 + I_2^2 + 2I_1 I_2 \cos \varphi) + k_3 I_b^2] \begin{bmatrix} dx \\ dy \end{bmatrix}$$

$$- \frac{1}{2} k_3 I_b^2 \begin{bmatrix} \cos 2(\omega t + \beta) & \sin 2(\omega t + \beta) \\ \sin 2(\omega t + \beta) & -\cos 2(\omega t + \beta) \end{bmatrix} \begin{bmatrix} dx \\ dy \end{bmatrix} \quad (18)$$

$$k_2 = \frac{9\mu_0 I_{Fe} r w_1^2}{8\pi \delta_0^3} \quad (19)$$

$$k_3 = \frac{9\mu_0 I_{Fe} r w_b^2}{2\pi \delta_0^3} \quad (20)$$

In comparison to equation (9) there are two additional components in equation (18). The first component in equation (18) is the same as equation (9). Both second and third components are dependent on the eccentricity of the rotor  $dx$  and  $dy$ .

In the third component of equation (18) the influence of  $dx$  and  $dy$  on  $F_x$  and  $F_y$  are coupled and their factors are sinusoidal function with twice the frequency of the current frequency. This means that the radial force generated from the superposition of the rotating fields consists of an alternative component which alternates twice within a period of the rotating field. For the geometrical parameters of the bearingless wound-rotor induction motor there exist  $k_1 > k_2 \gg k_3$ , and  $I_1, I_2 > I_b$ , the amplitude  $1/2 k_3 I_b^2$  of the alternative component is much smaller than the other components. Thus, the third component in equation (18) can be neglected.

Further it can be assumed that the radial force consists of two main components as following:

$$\begin{bmatrix} F_x \\ F_y \end{bmatrix} = k_1' I_\mu \begin{bmatrix} i_x \\ i_y \end{bmatrix} + [k_1 (I_1^2 + I_2^2 + 2I_1 I_2 \cos \varphi)] \begin{bmatrix} dx \\ dy \end{bmatrix}$$

$$= k_1' I_\mu \begin{bmatrix} i_x \\ i_y \end{bmatrix} + k_d \begin{bmatrix} dx \\ dy \end{bmatrix} = \begin{bmatrix} F_{ix} \\ F_{iy} \end{bmatrix} + \begin{bmatrix} F_{dx} \\ F_{dy} \end{bmatrix} \quad (21)$$

$$k_d = k_1 (I_1^2 + I_2^2 + 2I_1 I_2 \cos \varphi) + k_3 I_b^2 \quad (22)$$

Equation (21) indicates that the radial force of the bearingless wound-rotor induction motor can be described as a function of the bearing current and the eccentricity of the rotor. This equation is similar to the general equation of radial force of the magnetic bearing [8]. But here the influence of the eccentricity to the radial force which is described as factor  $k_d$  is not constant. As described in equation (22),  $k_d$  is a function of the currents regarding to the 4-pole field and the 2-pole field. As discussed before, the  $k_3 I_b^2$  is much smaller

than the other component, then  $k_d$  is mainly dependent on the currents of the 4-pole field. Additionally,  $k_d$  changes with the load since it is also a function of the rotor phase angle.

### NUMERICAL COMPUTATION

Since the generation of the radial force in bearingless motors results from the superposition of two fields with different numbers of pole pairs, the air gap field in the bearingless motors is asymmetrically distributed. If the rotor has eccentricity, the air gap is not constant and the multi-inductance of the motor is not constant neither. All these points can not be exactly taken into account with the calculation done with analytical methods. So it is necessary to use finite element method to study the radial force of the bearingless wound-rotor induction motor.

#### Finite Element Method

With the static finite element method only constant fields in the motor can be computed, which can not exactly simulate the generation of radial force in the bearingless induction motor, because all the fields in the induction motor are rotating field and the rotor rotates at a different speed from the rotating field. The transient finite element method makes it possible to compute the motor with rotating fields and rotating rotor. So it is possible to simulate the transient responses of the motor. And the computed radial force of the motor is more closely to the practice. In addition, the computation results with transient finite element method can illustrate the rotation of the flux distribution.

The principle of the radial force computation with transient finite element method was introduced in [5], where also the transient responses of the radial force and the torque were compared between the bearingless squirrel cage induction motor and the bearingless wound-rotor induction motor. In this paper some further results from the computation with transient finite element method for the bearingless wound-rotor motor are discussed.

#### Radial Force Without Rotor Eccentricity

First the motor is assumed to be at the center position and the influence of the rotor eccentricity will not be taken into consideration. Then the radial force was computed at different bearing currents, while the driving current keeps constant. In [5] it was already verified that the change of the bearing current has no influence on the driving part. So the total 4-pole field keeps constant. In Figure 2 it is shown that the radial force is

proportional to the bearing current. This result is coincided with equation (13).

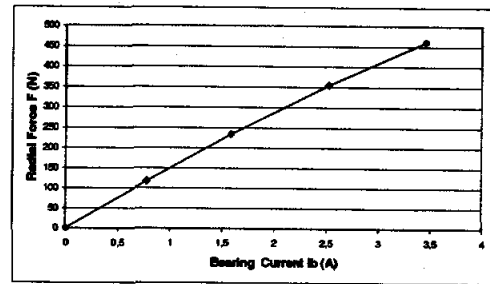


FIGURE 2: Radial force with bearing current

Further more the radial force and the torque were computed at different rotor speeds, while the bearing current keeps constant.

Figure 3 shows the results of the numerical computations. The torque increases with the increase of the slip, this relationship is the same as the theoretical torque speed characteristics of induction machines. It is also shown that the radial force keeps constant at different rotor speeds. In the computation the driving voltage is constant at different speeds, the driving current and the rotor current vary with the change of the speed, but the total 4-pole field keeps constant. On the other hand, the constant bearing current results in the constant 2 pole field. The result indicates that the value of the radial force is independent of the load. This is also coincided with equation (13).

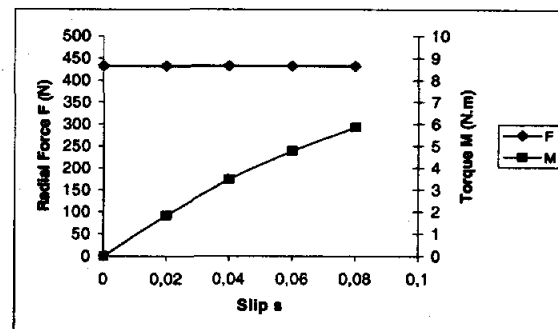
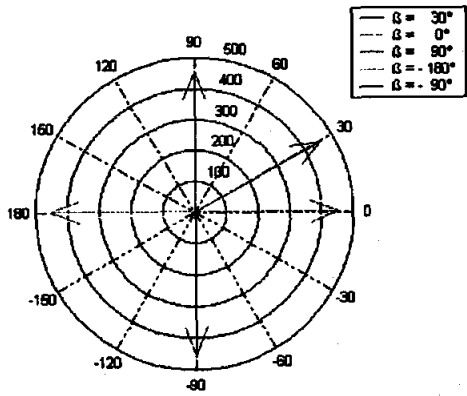


FIGURE 3: Radial force and torque with slip

To study the direction of the radial force further computations were carried out. From equation (15) it can be seen that the direction of the radial force  $\gamma$  is dependent on the phase angle between the bearing current and the driving current  $\beta$ . So it should be possible to change  $\beta$  to control the direction of the radial force.



**FIGURE 4:** Radial force direction with phase angle between the driving current and the bearing current

Figure 4 shows the direction of the radial force at different phase angles between the bearing current and the driving current  $\beta$ . For the first calculation with voltages added to the driving winding and the bearing winding, the resulted phase angle between the bearing current and the driving current  $\beta = 30^\circ$ , the radial force has an angle of  $30^\circ$ . If it is forced that  $\beta = 0^\circ$ , then the radial force is changed also in direction  $0^\circ$ . If the phase angle  $\beta$  decreases further with  $90^\circ$ , the direction of the radial force changes also to correspondingly  $90^\circ$ .

The four diagrams in Figure 5 show the flux distributions at the four different phase angles  $\beta = 0^\circ$ ,  $90^\circ$ ,  $180^\circ$  and  $-90^\circ$ , which results in the four typical directions of the radial force as show in Figure 4. So the direction of the radial force can be changed with the phase angle  $\beta$ .

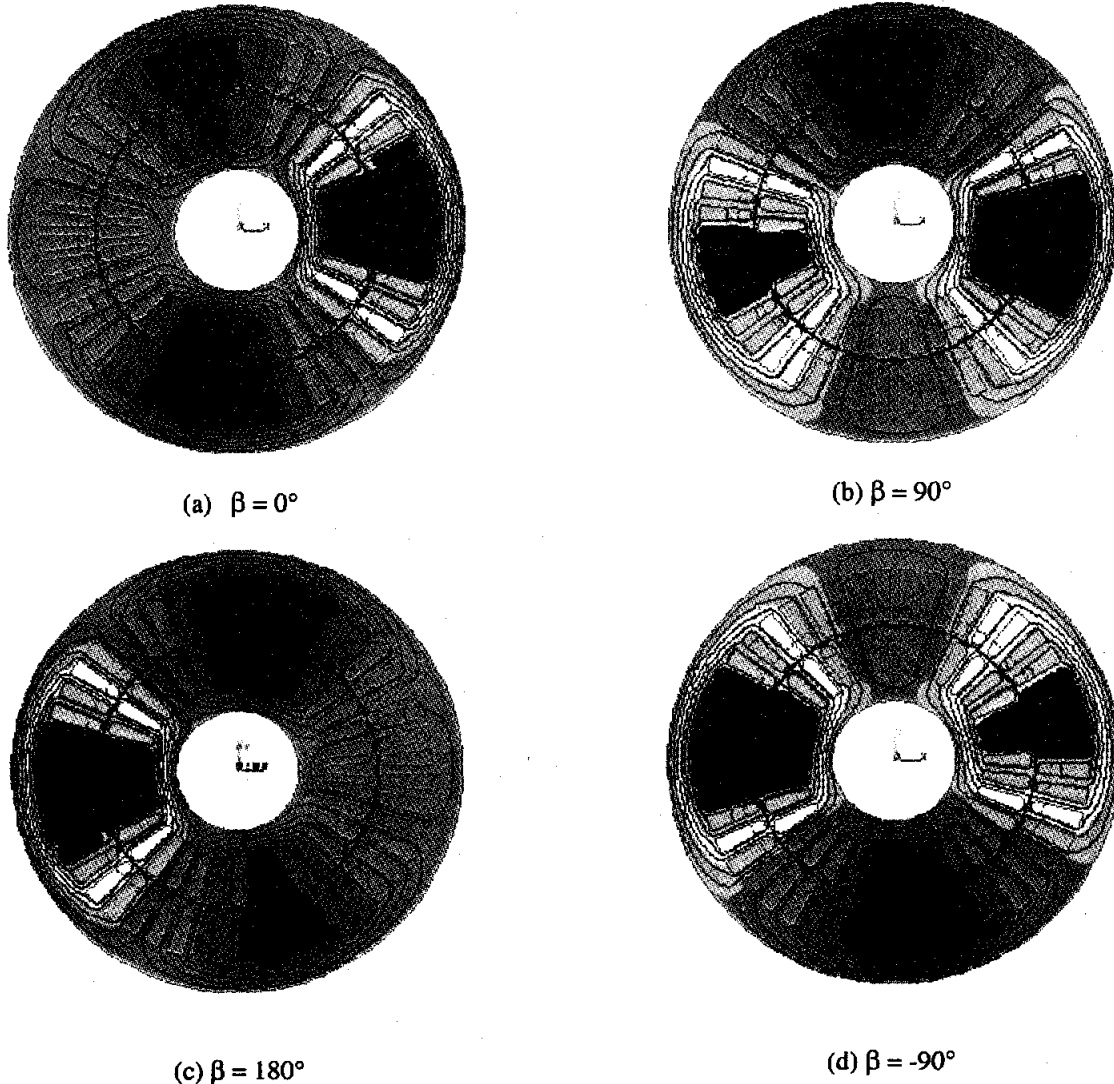


**FIGURE 5:** Rotating field and phase angle

### Radial Force With Rotor Eccentricity

With the transient finite elements methods the radial force of the bearingless wound-rotor induction motor was also computed at different rotor eccentricities. Figure 6 shows the radial force with rotor eccentricity  $dy = -0.1\text{mm}$ . At  $t = 0$ , only the driving winding is supplied with voltage, the radial force is mainly in negative y direction due to the eccentricity. But there is also a small radial force in x direction, because the multi-inductance of the motor is not constant, if the air gap is not constant. With the finite element method the change of the multi-inductance and the saturation of the motor can be taken into account.

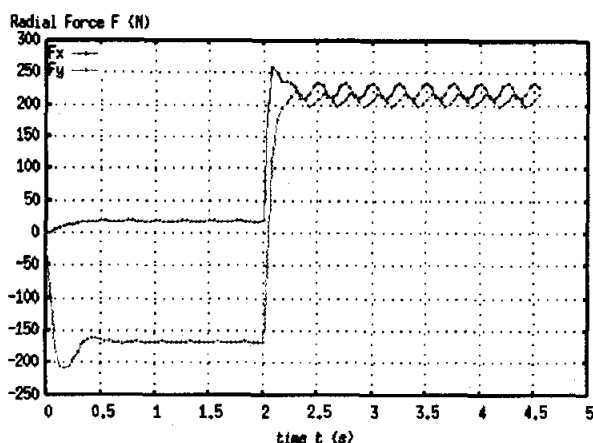


FIGURE 6: Radial force with  $dy=0.1\text{mm}$

At  $t = t_1$ , the bearing winding is also connected with voltage, then the radial force consists not only of the component due to the eccentricity, but also of the component generated from the bearing current. It can also be seen that the radial force consists of a constant component and an alternative component which has twice the frequency of the currents. This is coincided with equation (18). It is obvious that the amplitude of the alternative component is much smaller than the constant component.

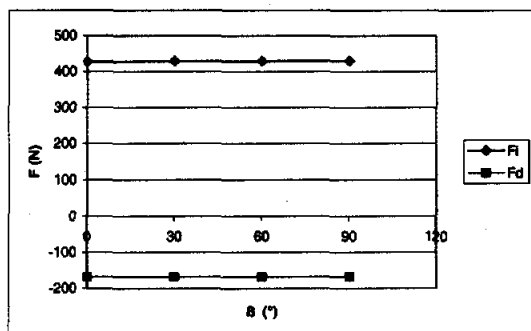


Figure 7: Radial force components at  $dy=-0.1\text{mm}$  with  $\beta$

Further computations with different phase angle  $\beta$  at different eccentricities were carried out. And the results in Figure 7 show that radial force due to the eccentricity  $F_{dy}$  is almost constant during the variation of the phase angle  $\beta$ . So it can be seen that the  $k_d$  is mainly dependent on the 4-pole field. Therefore, the simplified equation (21) is reasonable and can be used for the levitation control of the bearingless wound-rotor induction motor.

### CONCLUSION

The radial force of the bearingless wound-rotor induction motor was theoretically analyzed and studied with the transient finite element method. The radial force with no rotor eccentricity is proportional to the bearing currents and the direction of the radial force can be controlled by the phase angle between the bearing currents and the driving currents. The influence of the rotor eccentricity on the radial force is also studied.

### REFERENCES

1. A. Chiba, M. A. Rahman and T. Fukao, "Radial force in a bearingless reluctance motor", IEEE Transactions on Magnetics, Vol.27, No.2, pp. 786-790, March 1991
2. R. Schöb, "Beiträge zur lagerlosen Asynchronmaschine", Dissertation, ETH, Switzerland, 1993
3. Y. Okada, S. Miyamoto and T. Ohishi, "Levitation and torque control of internal permanent magnet type bearingless motor", IEEE Transactions on Control Systems Technology, Vol.4, No.5, pp. 565-571, September 1996
4. K. Ben Yahia, "Entwicklung von Magnetlagern am Beispiel einer linearen Magnetführung und einer lagerlosen Asynchronmaschine", RWTH Aachen, Germany, Dissertation, 2000
5. J. Cai, G. Henerberger, "Transient FEM Computation of Radial Force and Torque for Bearingless Wound-Rotor Induction Motors", Proceedings of the fifth International Conference on Electrical Machines and Systems, pp. 991-994, Shenyang, 2001
6. J. Cai, G. Heneberger, "Entkopplung des Antriebssystems vom Schwebesystem für lagerlose Asynchronmaschinen", Tagungsband 5. Workshop Magnetlagertechnik, pp. 115-122, Zittau, 2001
7. G. Henneberger, "Elektrische Maschinen II - Dynamisches Verhalten elektrischer Maschinen, Stromrichterspeisung, Regelverfahren", RWTH Aachen, Germany, February 1994
8. G. Schweitzer, A. Traxler, H. Bleuler, "Magnetlager", Springer-Verlag, 1993